Japanese Journal of Applied Physics

REGULAR PAPER

Estimation of viscoelasticity of radial artery via simultaneous measurement of changes in pressure and diameter using a single ultrasound probe

Japanese Journal of Applied Physics **59**, SKKE04 (2020) **REGULAR PAPER**
https://doi.org/10.35848/1347-4065/ab7f1c

Estimation of viscoelasticity of radial artery via simultaneous measurement of changes in pressure and diameter using a single ultrasound probe

Takumi Saito[1], Shohei Mori[2], Mototaka Arakawa[1,2*], Shigeo Ohba[2], Kazuto Kobayashi[3], and Hiroshi Kanai[1,2]

[1]*Graduate School of Biomedical Engineering, Tohoku University, Sendai 980-8579, Japan*
[2]*Graduate School of Engineering, Tohoku University, Sendai 980-8579, Japan*
[3]*Honda Electronics Co. Ltd., Toyohashi 441-3193, Japan*

*E-mail: arakawa@ecei.tohoku.ac.jp

Received December 4, 2019; revised January 21, 2020; accepted March 11, 2020; published online April 1, 2020

To establish an evaluation index for vascular endothelial function, we developed an ultrasonic probe that can measure changes in blood pressure and blood vessel diameter at the same position in the radial artery. Based on phantom experiments, the pressure waveforms measured using the piezoelectric effect of the ultrasonic probe element and those using a pressure sensor exhibited a high correlation (correlation coefficient: $r = 0.979 - 0.999$). We confirmed the continuous measurement of the relationship between changes in blood pressure and the diameter from the in vivo experiments. We could then estimate the changes in viscoelasticity by calibrating the output from the probe element to the absolute blood pressure values in advance. The average coefficients of variations were 0.02 and 0.24 for elasticity and viscosity, respectively. This study demonstrated the possibility of measuring changes in the viscoelastic moduli of the radial arterial wall due to flow-mediated dilation using the developed ultrasonic probe. © 2020 The Japan Society of Applied Physics

1. Introduction

Arteriosclerosis is a major cause of cardiovascular diseases. Several techniques are available for the diagnosis of arteriosclerosis, including intravascular ultrasound and X-ray imaging. However, these techniques are not suitable for repeated applications because of their invasiveness. Non-invasive diagnostic techniques to measure indices such as pulse wave velocity (PWV)[1,2] and ankle-brachial index[3] have also been proposed. However, since these indices are calculated only as the average value in a wide range of blood vessels, local changes in the vascular wall characteristics due to the progression of arteriosclerosis cannot be diagnosed. In addition, these parameters are applicable when the advancement of arteriosclerosis has progressed more than vascular endothelial dysfunction or changes in smooth muscle traits. Since vascular endothelial dysfunction and changes in smooth muscle traits are reversible,[4] diagnosis at an early stage is important. To diagnose arteriosclerosis at an early stage, it is important to evaluate vascular endothelial function.

Plethysmography and flow-mediated dilation (FMD) using ultrasound[5–7] are used as the main evaluation methods for vascular endothelial function. In plethysmography, vascular endothelial function is generally measured by inserting a catheter into the blood vessel to inject vasoactive substances,[8,9] and cannot be applied repeatedly due to its invasiveness. As a non-invasive technique, plethysmography measurements via ischemic reactive hyperemia also has been developed. In this method, instead of injecting vasoactive substances directly into a blood vessel, an increase in blood flow after the release of blood is measured. However, it has not been widely used in clinical practice due to limitations such as a low specificity.[10] FMD measurement has been widely recognized for its adoption in the Framingham Heart Study, and a large volume of clinical data has been accumulated on its correlation with various risk factors.[11,12] When blood flow increases after the release of blood, the vasodilator nitric oxide (NO) is produced from vascular endothelial cells that are stimulated by shear stress from the blood flow.[13] When NO acts on the medial smooth muscle, the vascular wall relaxes.[14] In an FMD measurement, the ratio of radial artery diameter after restoration and the resting diameter (%FMD) is calculated. In this case, the arterial diameter is determined by setting the boundary of the blood vessel wall based on ultrasonic A-mode or B-mode images. However, the distance resolution of the ultrasonic measurement is approximately 0.15 mm, even when a 10 MHz high-frequency probe is used. %FMD in healthy individuals is approximately 6% or more,[15,16] and if the vessel diameter is 3 mm, an error of 0.1 mm is equivalent to approximately 3%, which makes accurate diagnosis difficult.

However, the change in the maximum diameter is indirect, and is caused by the changes in the mechanical property associated with the relaxation of the blood vessel wall. If the mechanical property can be measured directly, this will prove to be a better evaluation index. In addition, it was reported that even when the vascular endothelial function was normal, the viscoelastic properties of the vascular smooth muscle changed with organic vascular smooth muscle changes, and the vasodilator response decreased.[17,18] It is important to measure the change in the viscoelasticity of the vascular wall during FMD measurement to distinguish between vascular endothelial dysfunction and organic changes in the vascular smooth muscle. Therefore, our group focused on changes in the stress and strain on the blood vessel wall caused by heartbeat.[19–22] Significant differences were observed in the elastic modulus, rather than the maximum diameter change after restoration from resting during FMD measurements. We proposed a new evaluation method for the vascular endothelial function to measure not only elasticity but also viscosity. However, this method cannot accurately evaluate the viscoelasticity of the vascular wall because the measurement positions on the blood vessel wall are different for strain and pressure. Sakai et al. proposed a method to measure blood pressure and blood vessel diameter at virtually the same position.[23,24] Blood pressure waveforms were then obtained from the pressure sensors placed on both sides of the ultrasonic probe, and the delay time from the ultrasonic probe to the pressure sensors was corrected using the PWV calculated from these waveforms. However, it is difficult to determine the time delay because the PWV changes with a change in blood pressure within a heartbeat. To measure the blood pressure and blood vessel diameter at the same position by using only an ultrasonic probe, we have demonstrated that the blood pressure waveform can be measured via the piezoelectric effect of the element of the ultrasonic probe.[25] Furthermore, we have developed an ultrasonic probe that can measure blood pressure and blood vessel diameter at the same position.[26]

In the present study, we first verified the accuracy of the blood pressure waveform measured based on the piezoelectric effect of the element in an ultrasonic probe. The accuracy was confirmed using a blood vessel phantom in an aquarium experiment system. We then measured the blood pressure using the developed ultrasonic probe on the radial artery in vivo. Since the blood pressure measured using the ultrasonic probe element is output as a voltage, the absolute value of this measurement must be determined by calibration using the systolic and diastolic blood pressures obtained using a sphygmomanometer for every beat. To apply this method to the FMD measurement, it is necessary to perform the calibration procedure to determine the absolute blood pressure values using only the first beat. Similar to a previous report,[27] we compared the blood pressure waveforms measured using the ultrasonic probe element and tonometry, and demonstrated that the calibration process to obtain the absolute value of the blood pressure waveforms was valid for only the first beat. In the present study, the changes in blood pressure and the diameter were measured simultaneously by continuously measuring the blood pressure, and the change in viscoelasticity of the blood vessel wall for each heartbeat was estimated from the relationship between the changes in blood pressure and the diameter.

2. Experimental methods

2.1. Setup of phantom experiment

To confirm the accuracy of the blood pressure waveforms measured using the ultrasonic probe element, we performed measurements on a silicone rubber tube that simulated a blood vessel. Figure 1 shows the experimental system. The blood vessel phantom was installed in a water tank that simulated the circulatory system, and a pulsation pressure was applied to its lumen using a pulsation pump unit (Tobi, HTJ-1000). The blood vessel phantom with an inner diameter of 7 mm, a wall thickness of 1 mm, and an Asker C hardness of 10 was used. The transmural pressure on the phantom wall and its waveform were measured using the ultrasonic probe (Honda Electronics), and the internal pressure waveform was measured using a pressure sensor (Kyowa, PS-1KC). To simulate the structure in which the radial artery is supported by the radius, a biological tissue phantom with an Asker C hardness of 15 and a thin plastic plate were placed under the blood vessel phantom. The ultrasonic probe was directly pressed against it while the short-axis image of the blood vessel phantom was observed.

A linear array probe with 192 elements was customized by separating one center piezoelectric element from the ultrasonic transmitter/receiver unit to measure the blood pressure. The blood pressure was obtained using the piezoelectric effect of the ultrasonic probe's element. The pressure waveform $P(t)$ measured using the ultrasonic probe element is described by the following equation in the low-frequency region.[26]

$$P(t) = \frac{c_{33}^{E}}{Re_{33}} \int_{0}^{t} V(\tau)d\tau, \tag{1}$$

where c_{33}^{E} is the elastic constant under a constant electric field condition, e_{33} is the piezoelectric constant, and $V(\tau)$ is the voltage generated in the resistance R. The obtained output shows the differential of the blood pressure waveform. Therefore, the blood pressure waveform was obtained by integrating the measured waveform. The output from the piezoelectric element was passed through an amplifier with a gain of 40 dB and a low-pass filter (NF, FV-665) with a cutoff frequency of 30 Hz, and then output to an oscilloscope.

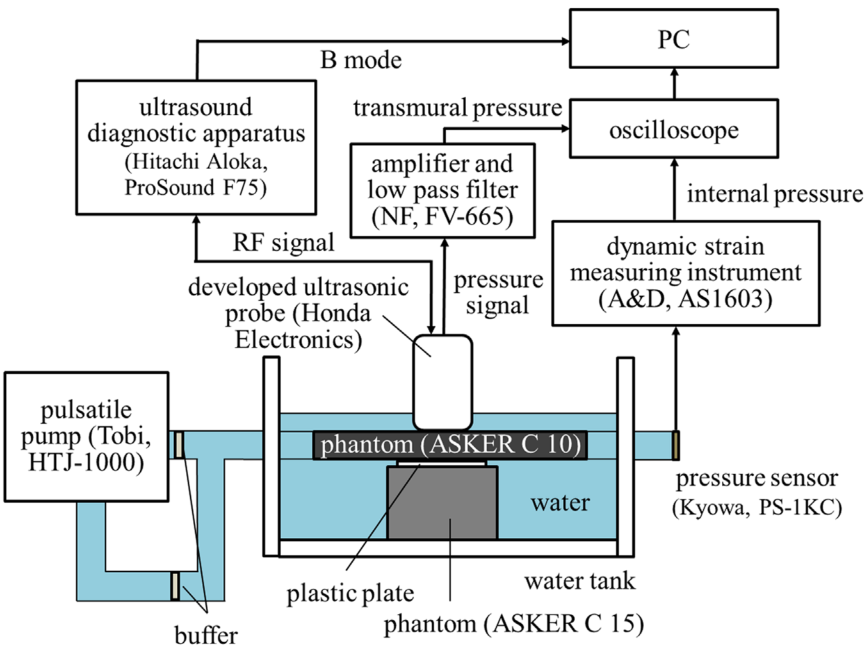

Fig. 1. (Color online) The experimental setting for the phantom experiment.

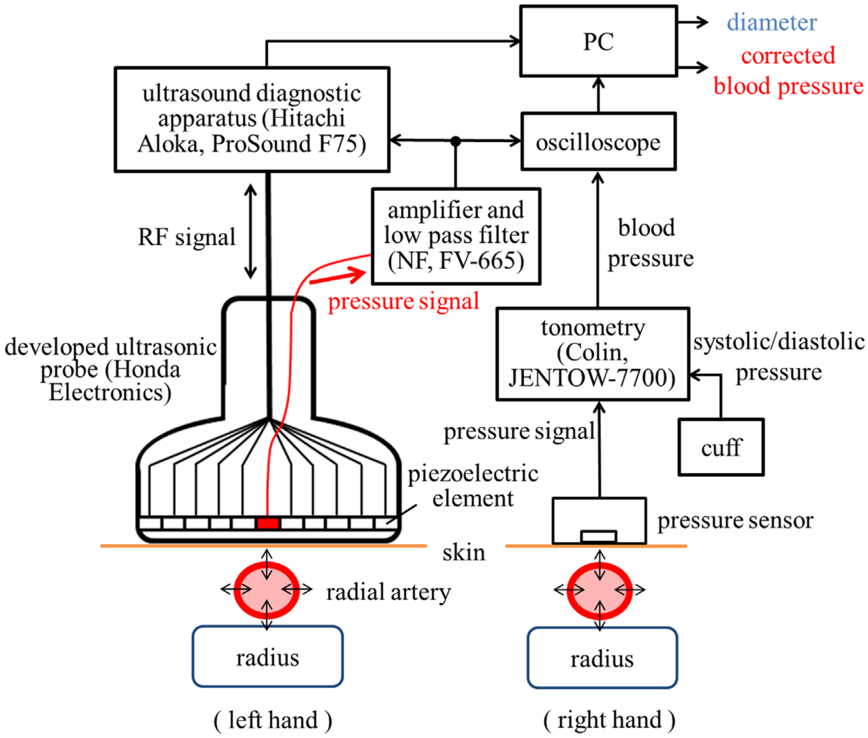

Fig. 2. (Color online) Schematic view of in vivo experiment.

The other 191 elements were used for the ultrasonic measurement. The probe was connected to an ultrasound diagnostic apparatus (Hitachi Aloka, ProSound F75). The measurement position was set so that the center of the probe was just above the blood vessel phantom while acquiring the B-mode image. The output signal acquired from the pressure sensor was passed through a dynamic strain measuring instrument (A&D, AS1603) and output to an oscilloscope.

To measure the blood pressure using an ultrasonic probe element, it is necessary to push down on the blood vessel to flatten the upper part. Therefore, we measured pressure waveforms while changing the force applied to the blood vessel phantom to investigate the influence of blood vessel shape on the blood pressure waveform. We then compared the pressure waveforms obtained for the ultrasonic probe and the pressure sensor.

2.2. Experimental setup for in vivo measurements

Figure 2 shows a schematic view of the experimental setting for in vivo measurements. The blood pressure and blood vessel diameter were measured at the left radial artery using the developed ultrasonic probe. The output from the piezoelectric element was passed through an amplifier with a gain of 40 dB, and a low-pass filter with a cutoff frequency of 30 Hz. The blood pressure waveform was then obtained by integrating the waveform. By utilizing the B-mode image as shown in Fig. 3, the measurement position was set so that the center of the probe was on the center of the radial artery. To acquire the blood pressure waveform, pushing pressure was applied from above the measurement position with the ultrasonic probe. The blood vessel diameter was measured at a center frequency of 7.5 MHz, a sampling frequency of 40 MHz, and a frame rate of 252 Hz. The phased-tracking method[28–31] was used to estimate changes in the diameter.

To obtain the values and waveforms of the blood pressure continuously, values and waveforms of the blood pressure were monitored on the right radial artery using tonometry (Nihon Colin, JENTOW-7700). An electrocardiogram (ECG) was also obtained. The subjects included three healthy males in their 20 s. Informed consent was obtained from the subjects and the study was approved by our institutional ethics committee for human research. All subjects were at least 2 h after meals and at least 30 min rest before the measurements. The measurements were performed in a sitting position at rest on each subject for 180 s at 60 s intervals.

Since the measured pressure is output as a voltage as indicated by Eq. (1), the absolute value was calibrated using the systolic and diastolic blood pressures obtained via tonometry. When the blood pressure waveform before calibration is $P(t)$, and the systolic and diastolic blood pressures measured by the tonometry are p_{sys} and p_{dias} respectively, the blood pressure waveform after calibration $\hat{P}(t)$ is given by:

$$\hat{P}(t) = \frac{p_{sys} - p_{dias}}{P_{max} - P_{min}}\{P(t) - P_{min}\} + p_{dias}, \quad (2)$$

where P_{max} and P_{min} are the maximum and minimum values of $P(t)$, respectively. Calibration to absolute blood pressures is necessary due to the effects of pressure attenuation in the subcutaneous tissue and the difference in the position, angle, and pressing force of the probe element on the radial artery at each measurement. However, considering the application of this method to FMD measurement, it is desirable not to calibrate to the absolute value at each heartbeat during the measurement. This is because there is a difference in blood pressure between the left and right arms after restoration. Therefore, the absolute value of the blood pressure waveform measured using the piezoelectric element of the ultrasonic probe was calibrated using p_{sys} and p_{dias} values obtained via tonometry only for the first heartbeat at the start of the

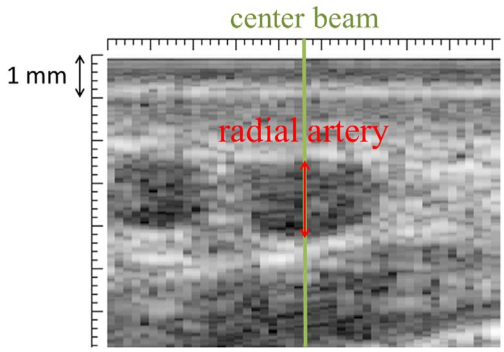

Fig. 3. (Color online) B-mode image of the left radial artery.

measurement. For subsequent heartbeats, $\hat{P}(t)$ was obtained by substituting $P(t)$ for each heartbeat into Eq. (2) using $p_{\rm sys}$, $p_{\rm dias}$, $P_{\max}$, and $P_{\min}$ of the first beat.

3. Results and discussion

3.1. Phantom experiment

Figure 4 shows the B-mode images of the blood vessel phantom, pressure waveforms obtained by the ultrasonic probe and a pressure sensor, and their correlations. From Figs. 4(a) to 4(c), the force on the blood vessel phantom from above by the ultrasonic probe increased. From the B-mode images, we confirmed that the phantom collapsed as the pushing force increased. Since the measurement positions of the ultrasonic probe and the pressure sensor were different, the time for the waveform obtained using the pressure sensor was adjusted so that the waveform rose with the same timing to compare the outline of the pressure waveforms to each other. The shapes of the pressure waveforms that were measured using the ultrasonic probe and the pressure sensor were in good agreement with each other and were highly correlated (correlation coefficient: $r = 0.979$–0.999). It was verified that the pressure waveform can be measured with high accuracy using the piezoelectric element of the ultrasonic probe, regardless of the shape of the blood vessel phantom.

3.2. In vivo experiment

Blood pressure waveforms were acquired using the ultrasonic probe and tonometry, for 5 consecutive beats for a duration of 180 s at 60 s intervals. Figure 5 shows the blood pressure waveforms at the start of the measurement and after 180 s. The delay time of the blood pressure waveform acquired by the ultrasonic probe caused by passing through a low-pass filter was corrected. For the blood pressure waveforms obtained from the ultrasonic probe element, the absolute values were obtained using the systolic and diastolic pressures obtained via tonometry only for the first beat, as shown

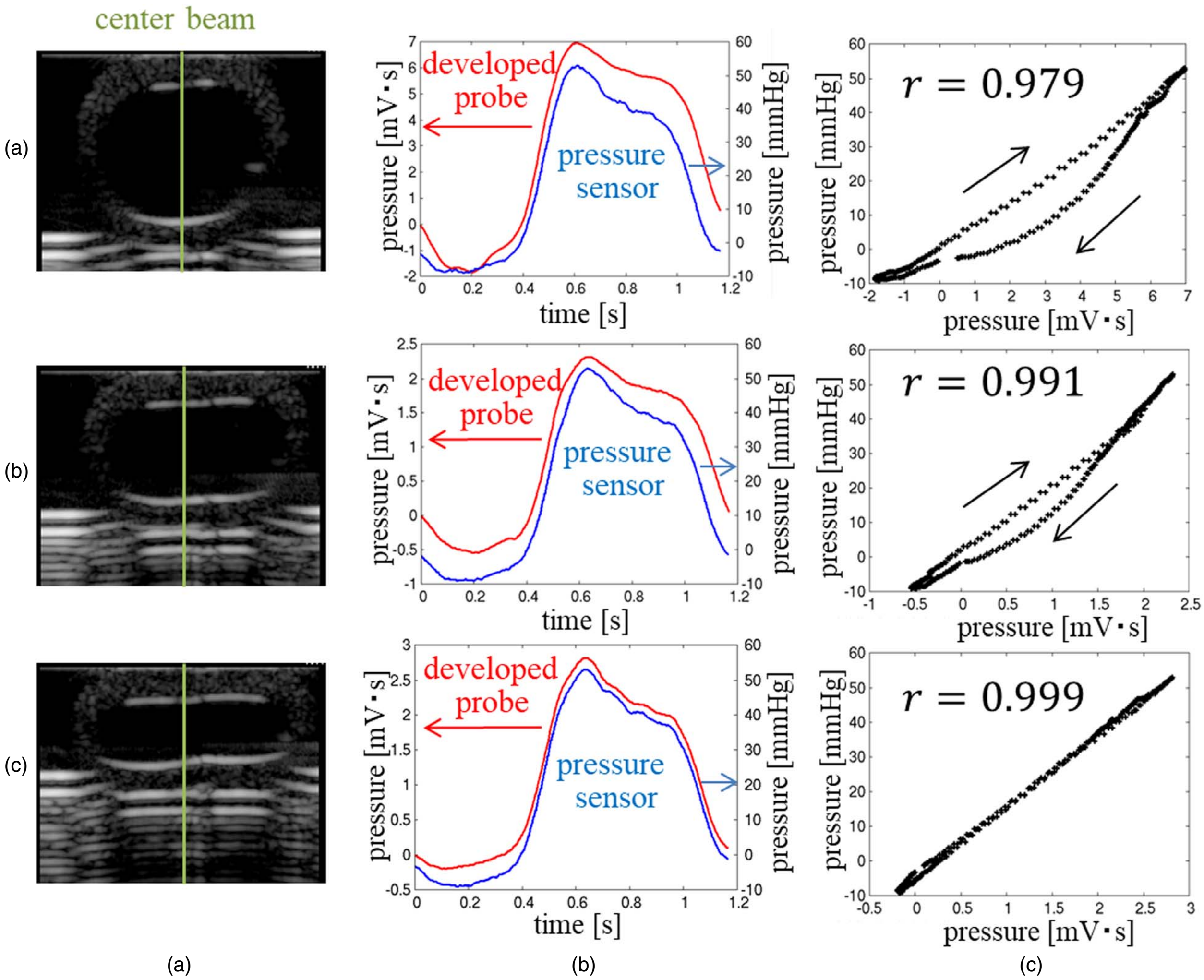

Fig. 4. (Color online) Results for the phantom experiment for (a) B-mode images of the blood vessel phantom, (b) comparisons of blood pressure waveforms measured using the ultrasonic probe element and a pressure sensor, and (c) correlations between the two pressure waveforms.

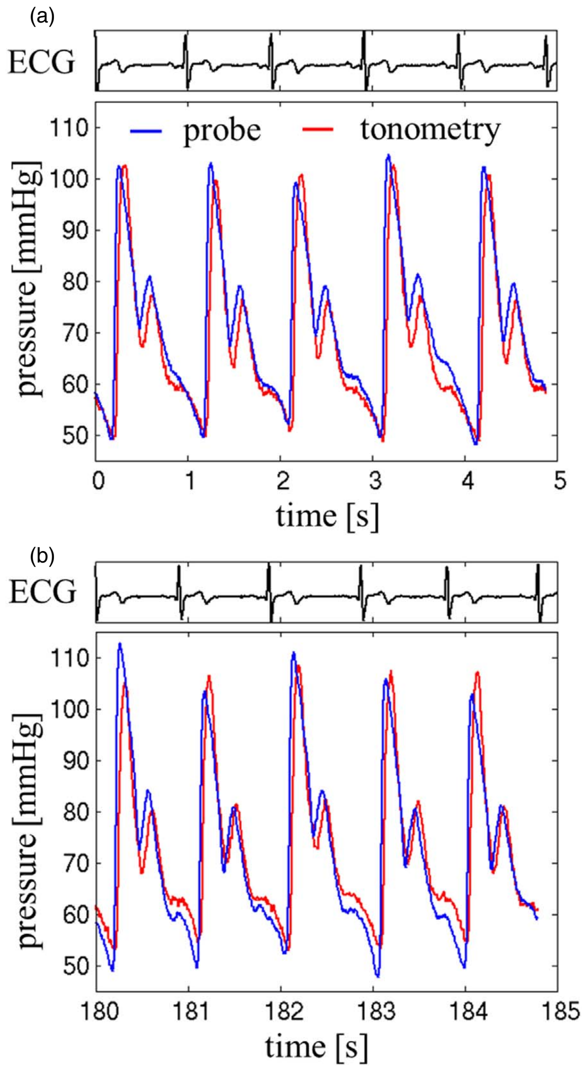

Fig. 5. (Color online) Blood pressure waveforms measured using tonometry and an ultrasonic probe (a) at 0 s (start of measurement) and (b) after 180 s.

in Fig. 5(a), and the relationship was used for the calibration of all other heartbeats. From Fig. 5(a), we confirmed that the blood pressure waveforms obtained from tonometry and the piezoelectric element of the ultrasonic probe were in good agreement for 5 consecutive heartbeats. In addition, they were almost identical even after 180 s according to Fig. 5(b). Figure 6 shows the changes in the systolic and diastolic pressures measured by tonometry and the ultrasonic probe. Each data point was the average of 5 consecutive beats. The blood pressure values that were measured using the ultrasonic probe element were close to those obtained using tonometry for 180 s. The maximum error of the systolic blood pressure as measured with the probe element was 3.5%, and that of the diastolic blood pressure was 8.1%. The pressure values acquired via tonometry were considered to be true readings.

The results suggest that stable measurements were realized because the position and the pressing force of the ultrasonic probe strongly affect the blood pressure waveform. By calibrating the blood pressure readings acquired using the piezoelectric element of the ultrasonic probe in advance, it was possible to continuously measure the blood pressure waveforms over several minutes.

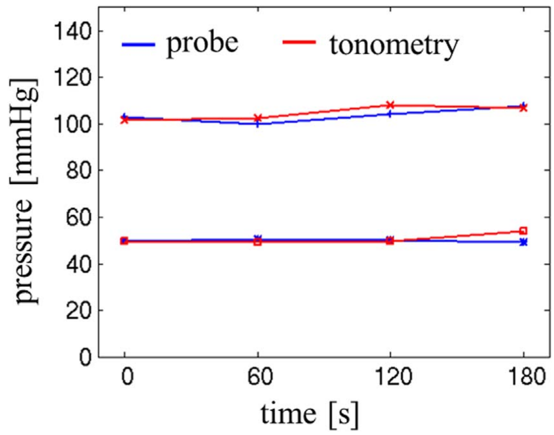

Fig. 6. (Color online) Temporal changes in systolic and diastolic blood pressures measured using the ultrasonic probe and a pressure sensor.

Subsequently, blood pressure waveforms and diameters were measured using a single ultrasonic probe. Figure 7 shows the relationship between changes in the blood pressure and the blood vessel diameter obtained for each heartbeat, separated by R-wave timing on the ECG for 3 consecutive heartbeats measured at 60 s intervals. B-mode images of the radial artery at the time of the R wave are also shown at the time of each data acquisition. Furthermore, the viscoelastic moduli were calculated for each beat, and the change over time is shown in Fig. 8. The viscoelastic moduli were calculated by applying a least square method using a Voigt model, which is a basic viscoelastic model for biological tissues.[32,33]

From the B-mode image and the relationship between the changes in the blood pressure and the blood vessel diameter as shown in Fig. 7, the position and shape of the blood vessel did not change significantly. As such, the stability of the measurement was confirmed. For Figs. 7(a) and 7(b), the minimum blood pressure changed approximately 4 mmHg, the maximum blood pressure changed approximately 5 mmHg, and a maximum deviation of the minimum diameter was approximately 0.02 mm during 3 heartbeats. Systolic and diastolic blood pressures are known to fluctuate with each heartbeat, and we confirmed that they fluctuated by several mmHg with each heartbeat by tonometry in Fig. 5. Therefore, the blood pressure shift in hysteresis is thought to be caused by normal physiological action, and the blood vessel diameter shift is caused by the blood pressure change. From Fig. 8(a), the elastic moduli estimation results showed little variation between heartbeats, and the average coefficient of variations (CV) between heartbeats was 0.02. The results also showed little variation over time, and the CV of the average value between time points was 0.06. These results demonstrated that we can measure changes in the elastic moduli of the blood vessel wall for at least 180 s. For the viscosity results shown in Fig. 8(b), the average CV between heartbeats was 0.24, and the CV of the average value between time points was 0.24. The variations in viscosity were larger than the variations in elasticity. The elastic modulus is related to strain, whereas the viscosity is related to the strain rate. Thus, it is likely to be affected by physiological action and slight body movements. The hysteresises shifted for 3 consecutive heartbeats in Figs. 7(a) and 7(b), and they were

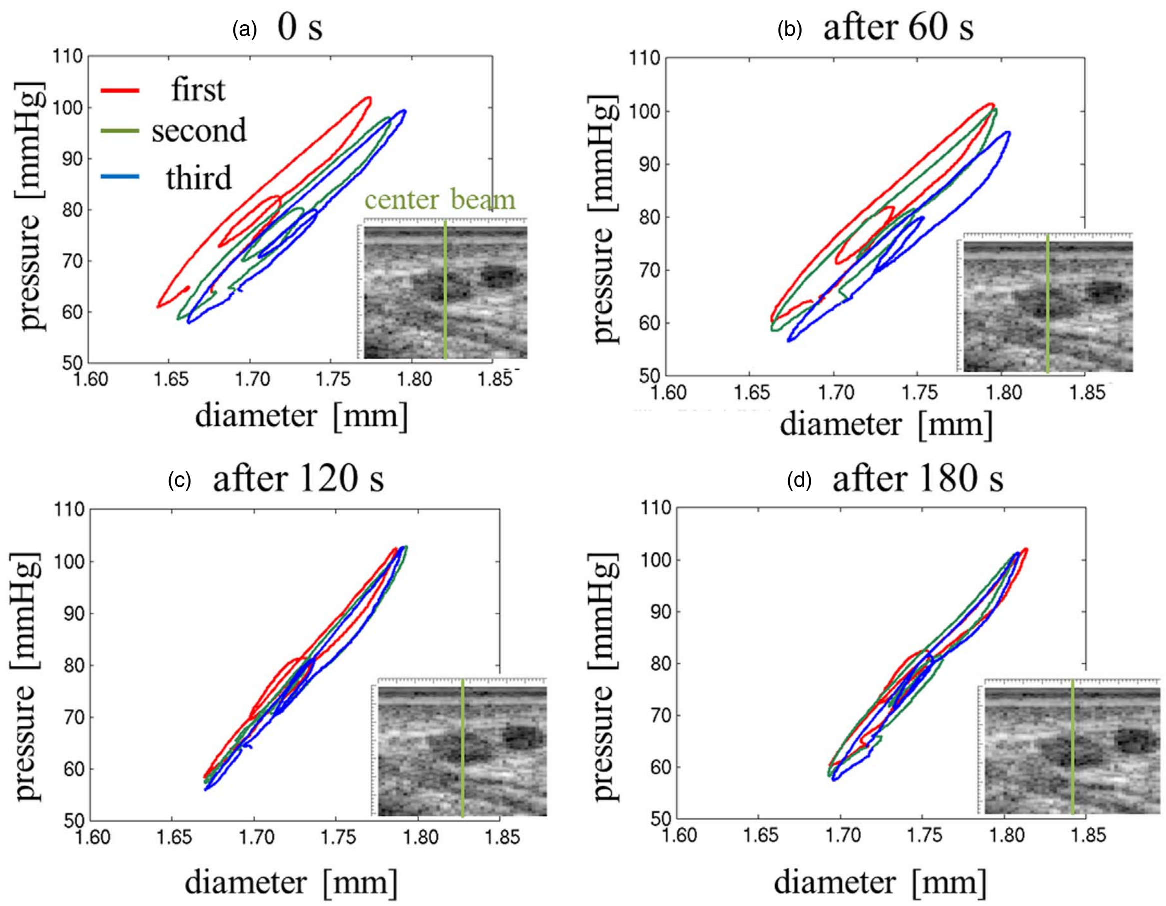

Fig. 7. (Color online) Relationship between changes in the blood pressure and the diameter of the blood vessel in B-mode images for 3 consecutive heartbeats (first, second, and third shown in figure) (a) at 0 s (start of measurement), (b) after 60 s, (c) after 120 s, and (d) after 180 s.

little change in Figs. 7(c) and 7(d). However, in Fig. 8, even when comparing the viscoelastic moduli at the times for Figs. 7(a)–7(d), the variations in 3 heartbeats were almost the same. This is because the slope of the hysteresis related to the elasticity and the area of the hysteresis related to the viscosity hardly changed. Therefore, it is considered that these changes among heartbeats have little effect on the estimated viscoelasticity.

Figure 9 shows the viscoelasticity estimation results for the three subjects. For all the subjects, the elasticity and viscosity were of the same order. Based on the results for the subjects, a relationship was not observed between the elasticity and the viscosity. Although the viscoelastic moduli that were estimated even at rest exhibited variations, it is considered to be within an appropriate range compared to the variations of the viscoelastic parameters at rest, in the experiments by Sakai et al.[24] and Kutluk et al.[34] In the experiment by Learoyd,[35] the elastic modulus of the carotid artery of young subjects was approximately 100–500 kPa in 50–130 mmHg, and the elasticity in Fig. 9(a) was smaller. This is because the radial artery, which is a blood vessel thinner than the carotid artery, is the target, and the blood vessel has an elliptical-cylinder shape because of the deformation of the blood vessel during measurement. When a blood vessel is elliptical, the diameter in the ultrasonic beam direction becomes smaller, and it is easy for the vessel to spread in that direction. As a result, the elastic moduli were estimated to be small. To address this problem, it is necessary to construct a viscoelastic model considering the shape of the blood vessel.

4. Conclusions

In the present study, we compared the pressure waveforms measured using an ultrasonic probe element and a pressure sensor for a blood vessel phantom, in the first instance. It was confirmed that the pressure can be measured with high accuracy regardless of the shape of the blood vessel phantom using the ultrasonic probe element.

Subsequently, it was shown that the blood pressure waveforms and blood pressure values can be continuously measured for several minutes by calibrating the output from the probe element to the absolute blood pressure values in advance. In addition, the blood pressure and the changes in the blood vessel diameter were measured simultaneously. In addition, the viscoelastic moduli of the radial arterial wall for each heartbeat were estimated based on the relationship between them. Similar experiments were conducted for the three subjects.

From these results, it was determined that we can continually measure the relationship between changes in the blood pressure and the blood vessel diameter to estimate changes in viscoelasticity using a single ultrasonic probe. To perform this measurement, it is necessary to calibrate the output from the probe element to the absolute blood pressure values at the start of measurements. This study demonstrates the possibility of measuring changes in the viscoelastic moduli on the radial arterial wall during FMD measurement using the developed ultrasonic probe.

In the future, by applying this method to FMD measurement, we intend to measure the temporal changes of the

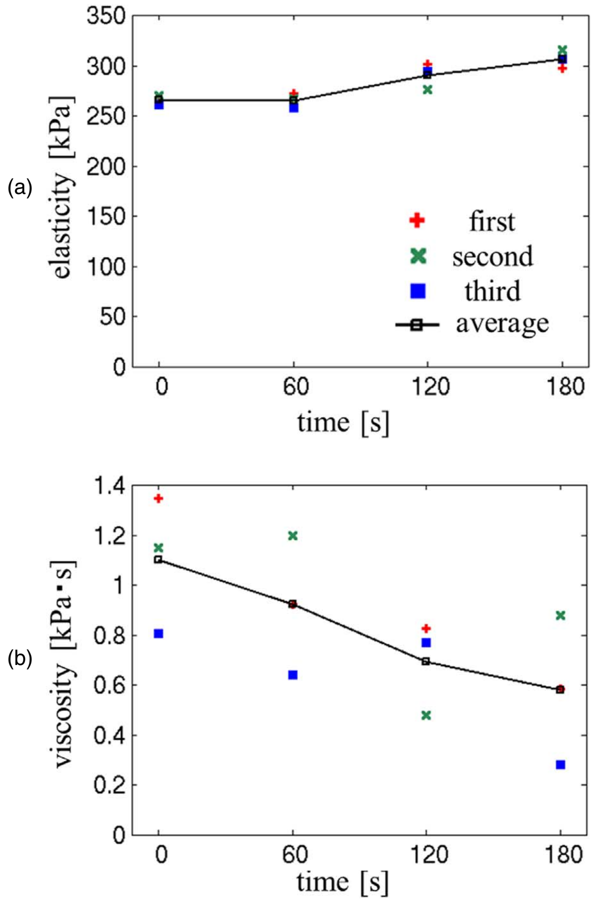

Fig. 8. (Color online) Temporal changes and their average over 3 consecutive heartbeats, (a) elasticity and (b) viscosity.

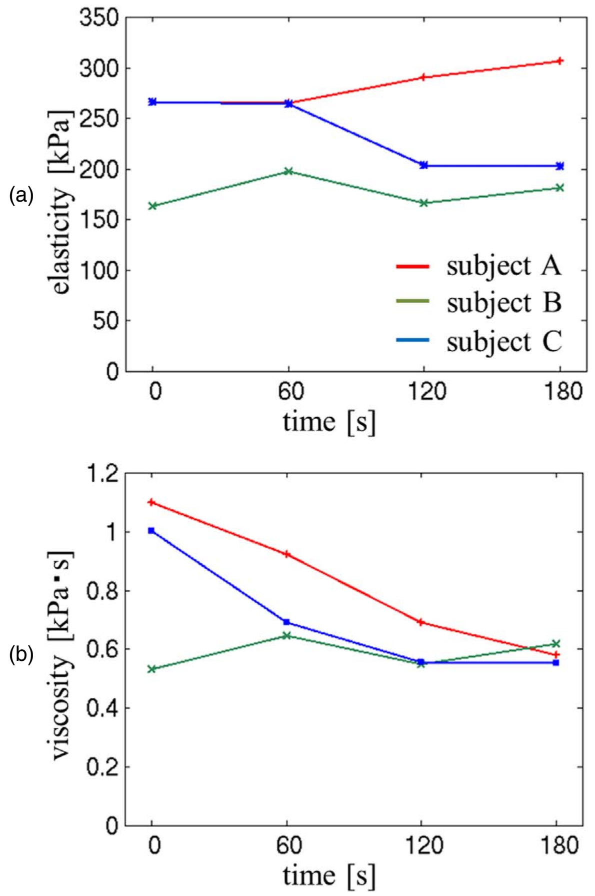

Fig. 9. (Color online) Temporal changes and their average over 3 consecutive heartbeats for 3 subjects, (a) elasticity and (b) viscosity.

viscoelastic moduli of the blood vessel wall, and to evaluate vascular endothelial function.

Acknowledgments

This work was partially supported by JSPS KAKENHI 19K22943.

1) E. Wetter and T. Kenner, *Grundlagen der Dynamik des Arterienpulses* (Springer, Berlin, 1968), p. 379 [in German].
2) D. A. McDonald, *Blood Flow in Arteries* (Edward Arnold, London, 1974) 2nd ed., p. 284.
3) J. I. Weitz, J. B. Chair, G. P. Clagett, M. E. Farkouh, J. M. Porter, D. L. Sackett, D. E. Strandness Jr., and L. M. Taylor, Circulation **94**, 3026 (1996).
4) R. Ross, New Engl. J. Med. **340**, 115 (1999).
5) M. C. Coretti et al., J. Am. Coll. Cardiol. **39**, 257 (2002).
6) N. M. Abdelmaboud and H. H. Elsaid, Egypt. J. Radiat. Nucl. Med. **44**, 237 (2013).
7) T. Nakamura et al., Int. J. Cardiol. **167**, 555 (2013).
8) J. A. Panza, A. A. Quyyumi, J. E. Brush Jr, and S. E. Epstein, New Engl. J. Med. **323**, 22 (1990).
9) Y. Higashi, S. Sasaki, K. Nakagawa, H. Matsuura, T. Oshima, and K. Chayama, New Engl. J. Med. **346**, 1954 (2002).
10) Japanese Circulation Society, *Guidelines for Non-Invasive Vascular Function Test*, (JCS 2013). In: JCS Joint Working Groups for guidelines for diagnosis and treatment of cardiovascular diseases 2013–2014 [http://j-circ.or.jp/guideline/pdf/JCS2013_yamashina_h.pdf] [in Japanese].
11) E. J. Benjamin, M. G. Larson, M. J. Keyes, G. F. Mitchell, R. S. Vasan, J. F. Keaney Jr., B. T. Lehman, S. Fan, E. Osypiuk, and J. A. Vita, Circulation **109**, 613 (2004).
12) H. Tomiyama, C. Matsumoto, J. Yamada, T. Teramoto, K. Abe, H. Ohta, Y. Kiso, T. Kawauchi, and A. Yamashina, Hypertens Res. **31**, 2019 (2008).
13) H. Iwasaki, M. Shichiri, F. Marumo, and Y. Hirata, Endocrinology **142**, 564 (2001).
14) R. F. Furchgott, Circ. Res. **53**, 557 (1983).
15) C. D. Black, B. Vickerson, and K. K. McCully, Dyn. Med. **2**, 1 (2003).
16) O. Rognmo, T. H. Bjrstad, C. Kahrs, A. E. Tjnna, A. Bye, P. M. Haram, T. Stlen, S. A. Slrdahl, and U. Wislff, J. Strength Cond. Res. **22**, 535 (2008).
17) Y. Matsuzawa, Nihon Rinsho **51**, 1951 (1993) [in Japanese].
18) K. Noma and Y. Higashi, Kessen to Junkan **19**, 311 (2011) [in Japanese].
19) K. Ikeshita, H. Hasegawa, and H. Kanai, Jpn. J. Appl. Phys. **47**, 4165 (2008).
20) K. Ikeshita, H. Hasegawa, and H. Kanai, Jpn. J. Appl. Phys. **48**, 07GJ10 (2009).
21) K. Ikeshita, H. Hasegawa, and H. Kanai, Jpn. J. Appl. Phys. **50**, 07HF08 (2011).
22) K. Ikeshita, H. Hasegawa, and H. Kanai, Jpn. J. Appl. Phys. **51**, 07GF14 (2012).
23) M. Sato, H. Hasegawa, and H. Kanai, Jpn. J. Appl. Phys. **53**, 07KF03 (2014).
24) Y. Sakai, H. Taki, and H. Kanai, Jpn. J. Appl. Phys. **55**, 07KF11 (2016).
25) M. Arakawa, K. Kudo, K. Kobayashi, and H. Kanai, Sens. Actuators A **286**, 146 (2019).
26) M. Arakawa, T. Saito, S. Mori, S. Ohba, K. Kobayashi, and H. Kanai, Sens. Actuators A **297**, 111487 (2019).
27) T. Saito, M. Arakawa, S. Mori, S. Ohba, K. Kobayashi, and H. Kanai, Proc. Symp. Ultrason. Electr. **40**, 1P5-2 (2019).
28) H. Kanai, M. Sato, Y. Koiwa, and N. Chubachi, IEEE Trans. Ultrason. Ferroelectr. Freq. Control **43**, 791 (1996).
29) K. Nakahara, H. Hasegawa, and H. Kanai, Jpn. J. Appl. Phys. **53**, 07KF09 (2014).
30) K. Tachi, H. Hasegawa, and H. Kanai, Jpn. J. Appl. Phys. **53**, 07KF17 (2014).
31) Y. Nagai, H. Hasegawa, and H. Kanai, Jpn. J. Appl. Phys. **53**, 07KF19 (2014).
32) J. Alastruey, A. W. Khir, K. S. Matthys, P. Segers, S. J. Sherwin, P. R. Verdonck, K. H. Parker, and J. Peiro, J. Biomech. **44**, 2250 (2011).
33) K. Niki, M. Sugawara, D. Chang, A. Harada, T. Okada, R. Sakai, K. Uchida, R. Tanaka, and C. E. Mumford, Heart Vessels **17**, 12 (2002).
34) A. Kutluk, T. Tsuji, M. Hamit, R. Nakamura, N. Saeki, Y. Higashi, M. Kawamoto, and M. Yoshizumi, J. Biomater. Tissue Eng. **5**, 334 (2015).
35) B. M. Learoyd and M. G. Taylor, Circ. Res. **18**, 278 (1966).